

Research Article

Removal of Color Scratches from Old Motion Picture Films Exploiting Human Perception

Vittoria Bruni, Paola Ferrara, and Domenico Vitulano

Consiglio Nazionale delle Ricerche, Istituto per le Applicazioni del Calcolo "M. Picone", Viale del Policlinico 137 00161 Roma, Italy

Correspondence should be addressed to Vittoria Bruni, bruni@iac.rm.cnr.it

Received 31 August 2007; Revised 8 April 2008; Accepted 15 July 2008

Recommended by Theodore Vlachos

In this paper a unified model for both detection and restoration of line scratches on color movies is presented. It exploits a generalization of the light diffraction effect for modeling the shape of scratches, while perception laws are used for their automatic detection and removal. The detection algorithm has a high precision in terms of number of detected true scratches and reduced number of false alarms. The quality of the restored images is satisfying from a subjective (visual) point of view if compared with the state-of-the-art approaches. The use of very simple operations in both detection and restoration phases makes the implemented algorithms appealing for their low computing time.

Copyright © 2008 Vittoria Bruni et al. This is an open access article distributed under the Creative Commons Attribution License, which permits unrestricted use, distribution, and reproduction in any medium, provided the original work is properly cited.

1. INTRODUCTION

The automatic detection and removal of degradation in film sequences is fundamental in the restoration process because of the huge number of the involved frames [1, 2]. To this aim, a really useful and effective restoration tool must involve oriented techniques that fully exploit the damage peculiarities. With regard to line scratches, different approaches have been proposed in the recent literature [1–13].

Scratches appear as straight lines lying on much of the vertical extent of the frame. They can have different color while their width is in a limited range of pixels [1]. They are often caused by a mechanical stress during the projection of a movie so that they occupy the same or quite the same location in subsequent frames. That is why they cannot be classified as temporal impulsive defects. In [5, 6] a physical model for the observed scratches has been provided by proving that they are caused by light diffraction. In fact, a scratch is a thin slit on the film material that it is crossed by the light during the projection and/or the scanning process. Since a different amount of the original information is removed in the degradation process, according to the depth of the slit, the damaged area can be modeled as a partially missing data region. Moreover, simple rules of the Human Visual System [14] can guide both the detection and the

restoration processes. In particular, the scratch is detected as a visible object in the scene and it is removed by shrinking its contribution till it becomes negligible for the observer. Based on these assumptions, the method in [5, 6] for black and white (BW) movies presents the following advantages: automation, low computational effort, good visual quality, and reduced number of false alarms [7].

Despite the variety of proposals for BW movies, little has been specifically done for color restoration. The objective of this paper is then to extend the model adopted for monochromatic frames in [5, 6] to color films. Nonetheless, the straightforward extension to each color channel does not work. In fact, color scratch has a different appearance in terms of size and transparency due to the structure of the film support. Moreover, more neighboring scratches with the same degree of visibility and the same vertical extension may appear. Finally, the relationship between the three color channels has to be accounted for in the restoration process in order to guarantee high-quality restored images. Hence, a more sophisticated generalization of the model for black and white film is proposed. It still exploits light diffraction, but it is made adaptive for suitably shaping the admissible scratches: red, blue, and white. Color movie restoration requires the simultaneous processing of the three color channels for each single frame, then the computational effort has to be controlled. To this aim, we propose a fast

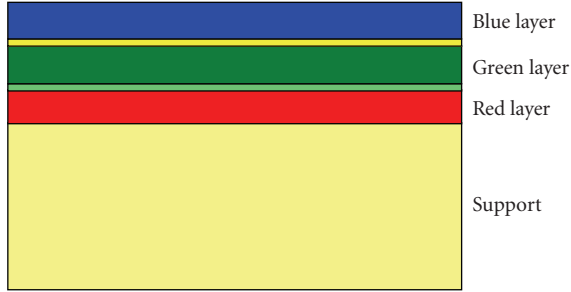


FIGURE 1: Structure of the color film support.

detection in the Magenta (M) channel of the CYMK color space, followed by an adaptive restoration in the RGB color space, according to the visibility of the defect. This strategy allows us to design a fast and automatic framework that is sufficiently independent of the knowledge of the various processes involved in the digitization of the film.

The paper is organized as follows. In Section 2 some discussions about color scratches are given while Section 3 contains the detection algorithm for BW frames and its extension to color ones. Section 4 presents the relative restoration while some experimental results along with comparisons with the state-of-the-art approaches are then presented in Section 5. Finally, Section 6 draws the conclusions.

2. COLOR SCRATCHES

Color film is based on the subtractive synthesis, which filters colors from white light through three separate layers of sensitive emulsions (see Figure 1). They are, respectively, sensitive to blue, green, and red. The printed images are then obtained using the synthesis of yellow, magenta, and cyan.

Accounting for the aforementioned process, it is theoretically possible to guess the color of the scratch according to the degradation under study. If the mechanism completely throws away information from the first layer of the frame support, the only information in the damaged area derives from magenta and cyan, and then the resulting scratch is blue. If also the second layer is damaged, the resulting image is cyan. Finally, if even the third layer is corrupted, information is completely lost: in this case a white scratch appears. This case is less frequent and it is the only one where pure inpainting-based restoration methods are necessary [15, 16].

Moreover, let Δ_S be the distance between the slit (scratch on the film material) and the screen (or lens of the projector). If λ is the wavelength of the light rays of the lamp while d_s is the observed scratch width on the screen, then a well-known diffraction rule gives the scratch's width d on the film material, that is,

$$d = \frac{2 \Delta_S \lambda}{d_s}. \quad (1)$$

Since $0.39 \mu\text{m} \leq \lambda \leq 0.78 \mu\text{m}$, the width of the scratch on the screen for the same slit d depends on the wavelengths that are



FIGURE 2: Degraded frame with three common types of scratch. From left to right: blue, red, and cyan.

allowed to pass through the slit. It is worth stressing that the aforementioned classification just considers cases where one or more than one layer has been completely removed by the projection mechanism. As a matter of fact, real scratches are often produced by a partial removal of the film material that gives them colors with different intensity and pureness.

In order to complete color scratches taxonomy, also red defects have to be considered. They may be caused in the very rare case where the mechanism acts on the opposite side of the support; in this case, it firstly removes the support and then the cyan layer providing a red scratch. However, it happens only after a traumatic stress of the film support that is very unusual. As a matter of fact, red scratches are mainly caused by the damage of intermediate negatives: if the yellow and magenta layers have been damaged, the cyan layer provides a printed image showing a red scratch on the resulting positive copy. It is evident that in this case, the diffraction is no longer valid. Nonetheless, it can be still used for modeling the analyzed defect because of its simplicity. It entails a sinc^2 behavior for the scratch that matches enough the real shape of the defect. In fact, scratches are characterized by a damped oscillating behavior whose main lobe contains most of the energy (see Section 3 for details).

Figure 2 shows a degraded frame having (from left to right) blue, red, and cyan scratches.

3. DETECTION

The main visible property of a line scratch is its geometry: it is a vertical line with limited width and significant energy. Therefore, it often represents a peak of the horizontal projection of the image: the *cross-section*, as shown in Figure 3. This latter is the Radon transform of the image that is computed along the vertical direction and corrected by its local mean [1, 5, 6]. The vertical extension and the significant energy in the horizontal *cross-section* are the main assumptions in the existing detection algorithms, as briefly described in the following.

A suitable combination of the Hough transform for detecting vertical lines and a damped sinusoid model for

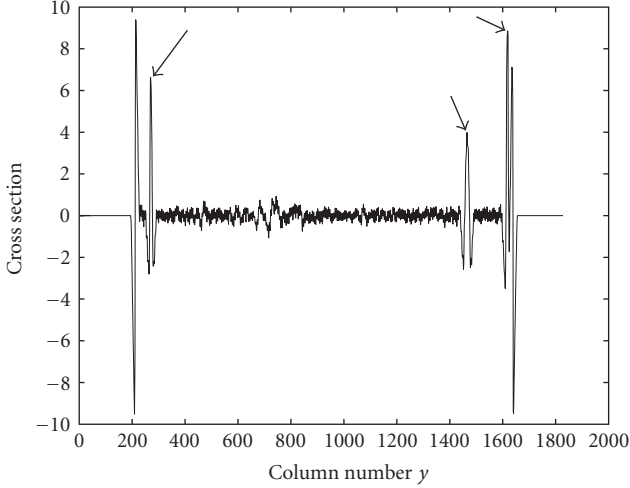


FIGURE 3: Horizontal cross section of the scratched image in Figure 2. Scratches are indicated by arrows. Their impulsive nature is evident.

the scratch horizontal projection is effectively exploited in [1]. The impulsive nature of the scratch is also used in [4], where it is detected in the vertical detail component of a wavelet decomposition, assuming a sinc shape for its horizontal projection. On the contrary, in [9, 10], scratches are characterized as temporal discontinuities of the degraded image sequence and then the Kalman filter is used for their detection. With regard to color scratches, it is worth mentioning the work in [12]: (intense) blue scratches are detected as maxima points of the horizontal projection of a suitable mask. The latter represents the enhanced vertical lines of the degraded image whose hue, saturation, and value amplitudes fall into predefined ranges.

The physical formation of a scratch on the film material has been considered in [5, 6]. It has been proved that the observed scratch derives from the diffraction effect. In fact, it is produced by the projector light that passes through the slit (i.e., the damaged region) of the film material. Therefore, the scratch appears as an area of partially missing data, where the original information has not completely been removed, according to the depth of the slit.

From now on we will, respectively, indicate with (x, y) the row and column of an image I . Therefore, for an $N_1 \times N_2$ image, $0 \leq x \leq N_1 - 1$ and $0 \leq y \leq N_2 - 1$. The contribution of a scratch over a fixed row \bar{x} of the degraded image $I(x, y)$ is modelled as follows:

$$I(\bar{x}, y) = (1 - (1 - \gamma)e^{(-2/m)|y-c_p|})G(\bar{x}, y) + (1 - \gamma)L_{\bar{x}}(y), \quad (2)$$

where $G(x, y)$ is the original image and $L_{\bar{x}}(y)$ is the 1D function model for the scratch, that is,

$$L_{\bar{x}}(y) = b_p \operatorname{sinc}^2\left(\frac{y - c_p}{m}\right), \quad (3)$$

according to the diffraction effect. Also, b_p , c_p , and m , respectively, are the maximum brightness, the location

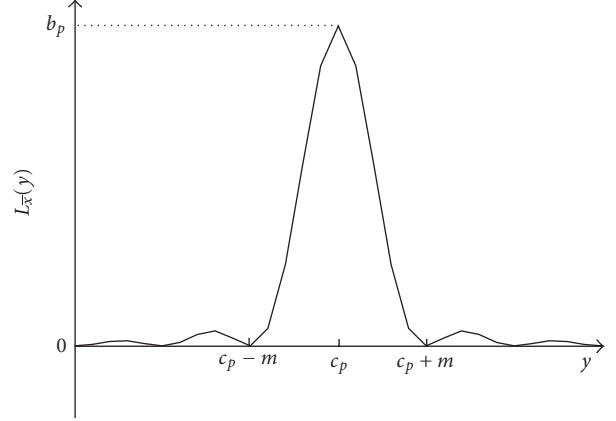


FIGURE 4: Sinc² shape of an ideal scratch on the horizontal cross-section of the degraded image, as in (3).

(column number), and the horizontal width of the scratch on the image, as depicted in Figure 4. However, γ is a normalization parameter that measures the global visibility of the scratch in the degraded image while $e^{(-2/m)|y-c_p|}$ approximates the positive decay of the scratch contribution from its central part toward its end. Moreover, γ compares the average energy of the peaks of the image with the one of the scratch and it is in the range $[0, 1]$; hence, the smaller γ , the more perceptible the scratch.

As (3) and Figure 4 show, the more y far from c_p , the less noticeable the scratch, while the significant energy of the defect is in the range $D = [c_p - m, c_p + m]$. For that reason, in (2) the amount of the original information in the degraded area is weighted by the decay of the scratch contribution and its degree of visibility over the whole image.

Since scratches are peaks of the horizontal *cross-section* of I , as shown in Figure 3, they can be detected among those peaks that subtend a sinc²-like shape, whose width is within a prefixed range and whose energy is appreciable enough to be visible in the local context of the analyzed scene. The detailed detection algorithm is given in Algorithm 1.

Notice that in the step 4(iii), only scratches whose intensity value over-exceeds the least perceivable one are selected. Algorithm 1 works for white scratches. For the black ones, it is necessary to invert the roles of maxima and minima points at step (2).

3.1. Fast color adaptation

In the detection of color scratches, each single color channel should be processed in order to detect the corresponding visible scratches. Nonetheless, this could increase too much the computational effort of the algorithm. According to the subtractive mechanism, the CYMK color space has been analysed and it has been observed that all scratches of the considered sequences appear in the magenta component as white lines (see Figure 5). Therefore, this color channel has been selected for performing a fast detection of the visible scratches over the whole color image, without specifying the color of the defect. This component allows in principle to

- (1) Compute the cross section \vec{c} of the scratched image I .
- (2) For each local maximum c_p of \vec{c} compute:
 - (i) the distance m from its closest left p_l and right p_r adjacent local minima, that is, $m = \lceil (p_r - p_l)/2 \rceil$;
 - (ii) the mean difference Δ_p between the corresponding amplitudes, that is,

$$\Delta_p = \frac{|\vec{c}(c_p) - \vec{c}(p_l)| + |\vec{c}(c_p) - \vec{c}(p_r)|}{2};$$
 - (iii) the area \mathcal{A}_p of the sinc^2 , as in (3), that better approximates \vec{c} in the least square sense in the interval $[p_l, p_r]$.
- (3) Compute the least perceptible intensity value \bar{b}_p for a scratch in the considered image using the Weber's law, that is, $\bar{b}_p = \frac{E}{0.98}$ [6], where E is the average of the energy values Δ_p used at step 2(ii).
- (4) Select the local maxima c_p such that
 - (i) m is in the range [3, 12];
 - (ii) Δ_p over-exceeds the average value E ;
 - (iii) \mathcal{A}_p over-exceeds the area of the sinc^2 defined in the interval $[p_l, p_r]$ with amplitude \bar{b}_p (The sinc^2 is the one in (3), where $b_p = \bar{b}_p$).
- (5) Store the found maxima locations in the set \vec{C} .

ALGORITHM 1: Algorithm for the detection of black and white scratches.

- Let I the RGB degraded image.
- (1) Critically subsample the image I by four along the horizontal direction and let I_d the downsampled image.
 - (2) Extract the magenta component M (in the CYMK color space) of I_d .
 - (3) Apply the detection algorithm for black and white scratches to M .

ALGORITHM 2: Algorithm for the detection of color scratches.

further reduce false alarms—if compared to a multichannel-based approach.

From empirical observations, it has been derived that the width of color scratches is in the range [3, 30] pixels, for images at resolution 2 K, that is, 1828×1462 pixels. The range above is greater than the one used for the BW model [1] because of the change of resolution. Therefore, the impulsive nature of the scratch may be penalized, especially in presence of significant transparency in correspondence to highly textured areas. In this case, the underlying information may produce little and spurious peaks in the cross-section that can alter detection results—see Figure 6(a). To overcome this problem, a suitable down-sampling can be applied along the columns direction. Scratches are more impulsive after this operation and the detection is faster. However, the sampling operation must reduce the allowed width of the scratch without destroying its shape. For that reason, the degraded image has been critically subsampled according to the Shannon-Whittaker theorem. For the analyzed sequence, we have empirically found that a good tradeoff is achieved by critically subsampling by 4—see Figure 6(b).

The detection algorithm, which has been described in Algorithm 1, is then applied to the critically subsampled magenta (M) component of the analyzed frame I , as it is described in Algorithm 2. Such a procedure results appealing for the involved speed up: just one subsampled channel (Magenta) has to be processed. The output of the detection phase consists of the vertical regions of the image that contain scratches.

4. RESTORATION

Most of the restoration approaches are based on the assumption that regions affected by scratches do not contain original information [1, 2, 4, 7–9, 11, 15, 16]. Hence, they try to propagate neighbouring clean information into the degraded area. The neighboring information can be found in the same frame [1, 4, 11, 15, 16] or also in the preceding and successive frame exploiting the temporal coherency, as done in [7–9].

The propagation of information can be performed using inpainting methods, as in [15, 16], or interpolation schemes [17]. With regard to this point, different approaches have been presented. In [1], an autoregressive filter is used for predicting the original image value within the degraded area. On the other hand, a cubic interpolation is used in [11], by also taking into account the texture near the degraded area (see also [2] for a similar approach), while in [4] low- and high-frequency components of the degradation are differently processed. Finally, in [7] each restored pixel is obtained by a linear regression using the block in the image that better matches the neighborhood of the degraded pixel.

However, scratches often remove just part of information, as it has been argued in Section 3. For that reason, in [13] an additive multiplicative model is employed. It consists of a reduction of the image content in the degraded area till it has the same mean and variance of the surrounding information. With regard to only blue scratches, in [12] removal is performed by comparing the scratch contribution in the blue- and green-color channels with the red one; the

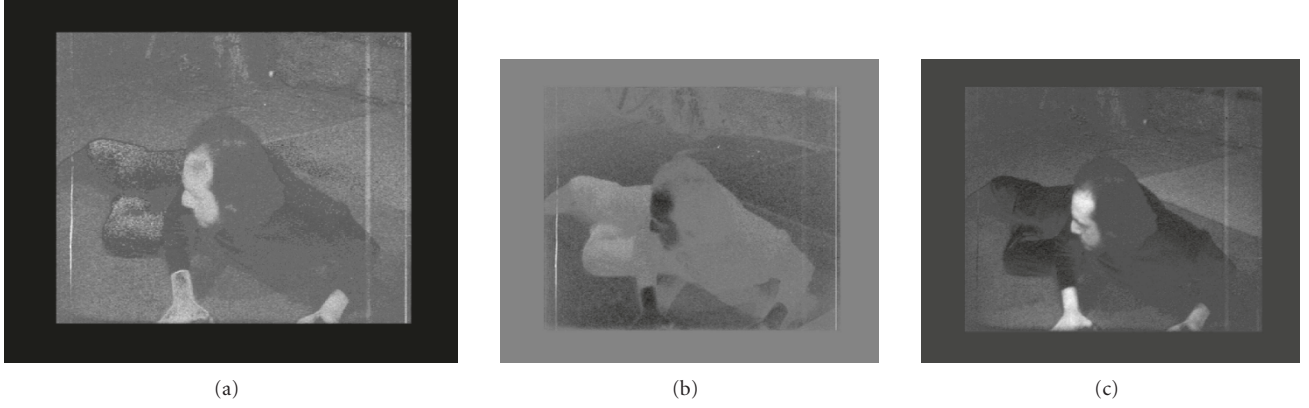


FIGURE 5: (a) Magenta component of the image in Figure 2. The three scratches are visible as bright defects. (b), (c) Chroma components (Cb and Cr, resp.) of the YCbCr color space: the three scratches are differently perceived. In particular, the red scratch is slight in the Cb component while the blue scratch leaves a black line in the Cr component.

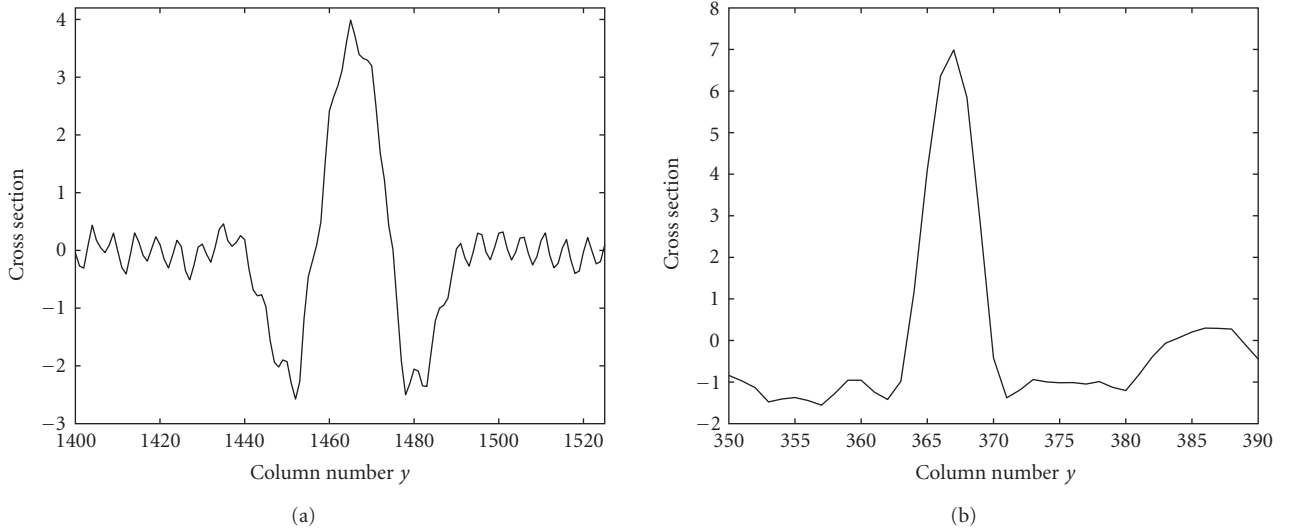


FIGURE 6: (a) Cross-section in the neighborhood of the red scratch in Figure 2 of the original degraded image—the high frequency may alter detection results since they depend on the local extrema of the signal. (b) Cross-section of the same scratch derived from the original image critically sampled by four: the shape of the scratch is evident and it is well defined by the model in (3). Notice that the length of the critically subsampled signal is 1/4 of the full length signal.

assumption is that the contribution of scratches in the red channel is negligible or completely misses.

Taking into account the model used in the proposed detection, the degradation can be removed by attenuating its contribution till it is masked by the original image [5]. The restoration is performed in the wavelet domain using biorthogonal symmetric filters H , G , \tilde{H} , \tilde{G} in an undecimated decomposition. H and G , respectively, are the lowpass and highpass analysis filters of the subband coding, while \tilde{H} and \tilde{G} are the corresponding low- and highpass synthesis filters. The multiscale decomposition allows to better remove the scratch from the lowpass component $AI(x, y)$ of the degraded image. In fact, the shape of the scratch better fits the data since it becomes more regular. Then, the estimation of

the scratch parameters, such as amplitude and width, is less sensitive to local high frequencies. In the vertical highpass component $VI(x, y)$ of the degraded image, the attenuation corresponds to a reduction of the contrast between the degraded region and the surrounding information at different resolutions, exploiting the semitransparency model. The attenuation coefficients are derived by inverting the equation model (2) and by embedding it in a Wiener filter-like scheme, where the noise is the scratch, that is,

$$w(\bar{x}, y) = \frac{(AI(\bar{x}, y) - C_2AL_{\bar{x}}(y))^2}{(AI(\bar{x}, y) - C_2AL_{\bar{x}}(y))^2 + ((C_2/C_1)AL_{\bar{x}}(y))^2} \quad \forall y \in D, \quad (4)$$

- Let \bar{C} the set of detected scratches. For each element $\tilde{c}_p \in \bar{C}$:
- (1) select the color component (among R, G, B) whose cross section has the highest value in correspondence to \tilde{c}_p ;
 - (2) adapt the scratch position to the full image dimension, that is, $c_p = 4\tilde{c}_p$;
 - (3) compute the undecimated wavelet decomposition of the selected component up to $J = \log_2(m/s_H)$ scale level, where s_H is the support length of the low pass filter associated to the employed wavelets basis and m is the estimated scratch width. Let $\{A_j, \{V_j\}_{1 \leq j \leq J}\}$ respectively be the low and high pass sub-bands of the decomposition;
 - (4) apply the restoration algorithm to each sub-band of the decomposition as follows:
for each row \bar{x}
 - (a) estimate the amplitude b_p in the least squares sense of the scratch shape at the considered band using (5) and the scratch domain at the coarsest resolution J , that is, $D = [c_p - 2^{(J-1)}m, c_p + 2^{(J-1)}m]$;
 - (b) compute the filter coefficients $w(\bar{x}, y)$, $\forall y \in D$ as defined in (4), suitably adapted to the considered sub-band;
 - (c) apply $w(\bar{x}, y)$ to the analyzed row:

$$\begin{aligned} \tilde{V}_j(\bar{x}, y) &= w(\bar{x}, y)V_j(\bar{x}, y) && \text{vertical details} \\ \tilde{A}_j(\bar{x}, y) &= w(\bar{x}, y)(A_j(\bar{x}, y) - \mathcal{M}_A) + \mathcal{M}_A && \text{low pass band,} \end{aligned}$$
 where \mathcal{M}_A is the local average of the low pass sub-band $A_j(\bar{x}, y)$ in the horizontal neighborhood Ω of the scratch domain D , that is, $y \in \Omega = [c_p - 2^{(J-1)}m - s_H, c_p + 2^{(J-1)}m + s_H]$.
- Invert the wavelet decomposition using the restored bands and let \tilde{I} be the resulting partially restored image;
- (5) extract the luminance component of \tilde{I} and evaluate the energy value in correspondence to c_p in the cross section of this component, as done at step 2(iii) of the detection algorithm. Compare it with the least admissible energy for a visible scratch, as in steps (3) and 4(iii) of the detection algorithm.
If the scratch is still visible, go to step (1) and apply the algorithm to the remaining color channels; else stop.

ALGORITHM 3: Restoration.



FIGURE 7: Restored frame in Figure 2 using the proposed algorithm.

where $AL_{\bar{x}}(y)$ is the lowpass component of the function in (3), $C_1 = (1 - (1 - \gamma)e^{(-2/m)|y - c_p|})$, $C_2 = (1 - \gamma)$, and D is the scratch domain. Notice that C_1 and C_2 are derived from (2). Moreover, (4) can be simply adapted to the vertical detail bands if VI and $VL_{\bar{x}}$ are considered instead of AI and $AL_{\bar{x}}$. The shrinkage coefficients $w(\bar{x}, y)$ measure a sort of signal-to-noise ratio, so that the scratch contribution is attenuated according to its local contrast with respect to the original information. In order to make this measure more precise, the algorithm is adapted at each row of the analyzed subband. In fact, the location of the scratch could slightly change from a row to another one, while the detection parameters, such as the amplitude b_p and the location c_p , are influenced by the down-sampling. Therefore, the algorithm firstly corrects the global detection parameters, that is, location of the maximum, width, asymmetry (resp., indicated by b_p , c_p , m)

according to the local information. In particular, b_p can be estimated from the data, minimizing the mean-square error in the scratch domain $D = [c_p - m, c_p + m]$, that is,

$$b_p = \min_{\alpha \in \mathbb{R}} \sum_{y \in D} |AI(\bar{x}, y) - \alpha AS_{\bar{x}}(y)|^2, \quad (5)$$

where $AS_{\bar{x}}(y) = \text{sinc}^2(|y - c_p|/m) * H$ is the function model for the lowpass component of a sinc^2 shape. Sob_p is then the peak value of the sinc^2 function that better matches, in the least-square sense, with the data at the considered resolution.

The perception of the defect can also be used to establish the order of the restoration of the three color channels. In fact, the removal of the defect in color images is usually performed in each color channel (R, G, B) independently. In order to minimize the computational effort and to avoid color artifacts, scratch removal can be performed in a hierarchical way: from the channel where scratch has the main contribution (the highest energy) to the one where it is less visible. The removal of the scratch from the first channel is followed by a visibility check on the luminance component, using the perception measures (based on *Weber's law*) of the detection step. More precisely, the energy of the scratch in the degraded region is compared with the minimum energy allowed for a visible object in the luminance component. If it is still visible, that is, the energy over-exceeds the threshold value, then the restoration algorithm on the successive channel is applied. Otherwise, the restoration process for the analyzed scratch stops. In this way, if the contribution of a scratch in a color channel is negligible for the human perception, any restoration process is performed.

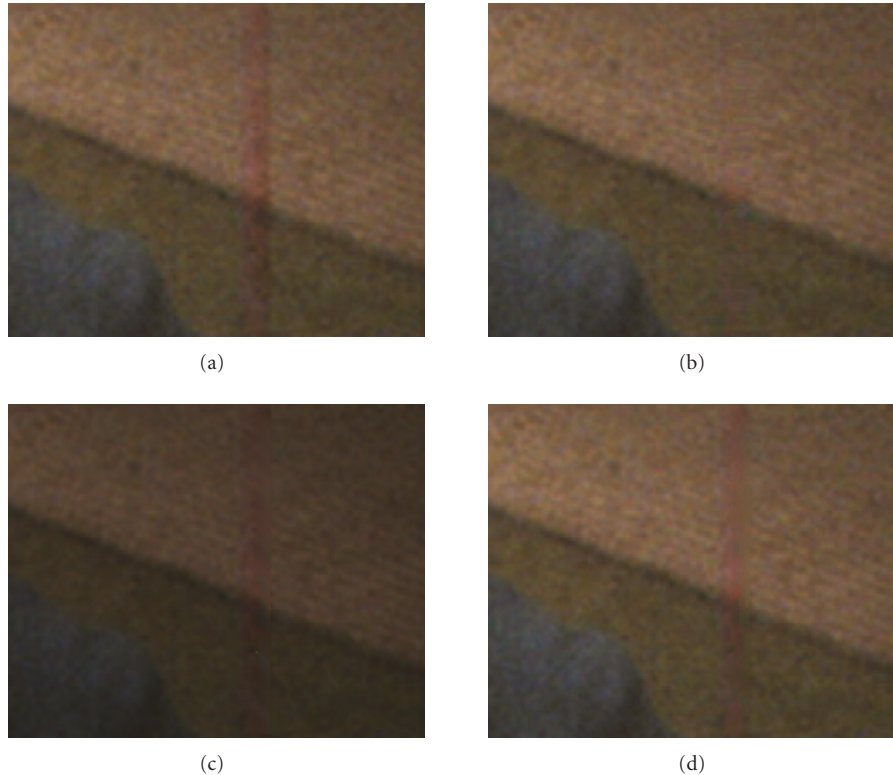


FIGURE 8: Zoom of the red scratch in Figure 2(a) restored using the proposed algorithm (b), the method in [1] (c) and the method in [7] (d).

4.1. The algorithm

In Algorithm 3, a general sketch of the whole restoration algorithm is given.

5. EXPERIMENTAL RESULTS

The algorithm has been tested on several real sequences (digitized copies of actual damaged films) having different subjects and of 1-2 minutes length (1500–3000 frames). In this paper we have shown some results concerning the sequences extracted from the film *Io sono un autarchico* (1976), kindly provided by Sacher Film s.r.l.. In order to check the visual quality of the results, some of the digital restored sequences have been copied back on film.

The detection algorithm has been performed on the cross-section of the magenta component of the image critically subsampled by 4. All scratches in the analyzed frames are selected with a few (or without) false alarms.

The undecimated wavelet transform using the biorthogonal 5/3 Le Gall filter has been used in the restoration algorithm, while the scale level depends on the width m of the scratch. In particular, it is $\log_2(m/s_H)$, where m is estimated in the detection step and s_H is the support of the lowpass analysis filter associated to the adopted wavelet basis. LeGall wavelets (5/3) are employed since they are symmetric and the support length of their analysis filters well matches with the admissible width for a scratch.

As it can be observed in Figure 7, the visual quality of the restored image is satisfying. In fact, scratches are removed without introducing artifacts both in the image content and, especially, in color information (some results are available at http://www.iac.rm.cnr.it/~vitulano/ext_model.htm).

The proposed framework has been compared with the algorithms in [1, 12] since they deal with one frame at a time. This cannot be considered a restriction. In fact, the initial condition of temporal detectors is the output of a spatial detector, as in [3, 7]. In particular, it is worth mentioning that the visibility-based detector in [6] has been employed in [7] since its competitive detection performances and for its ability in false alarms rejection.

For the analyzed sequences, we notice that the method in [1] fails in the detection of slight scratches while the one in [12] only works for very intense blue scratches, as the one in the leftmost part of the image in Figure 2.

Figure 8 shows the restoration results in correspondence to the red scratch: the texture of the carpet is preserved by the proposed algorithm while smoothing is introduced by the algorithms in [1, 7]. This is possible thanks to the adaptivity of the attenuation filter in (4) to the local image content, inside and outside the degraded region, even in presence of a diagonal edge. In fact, the algorithm works row by row. It separately processes the low and the high frequency of the degraded region, exploiting the physical model of the defect. It is worth stressing that the red scratch is wider than the classical black and white ones and it seems to lose the

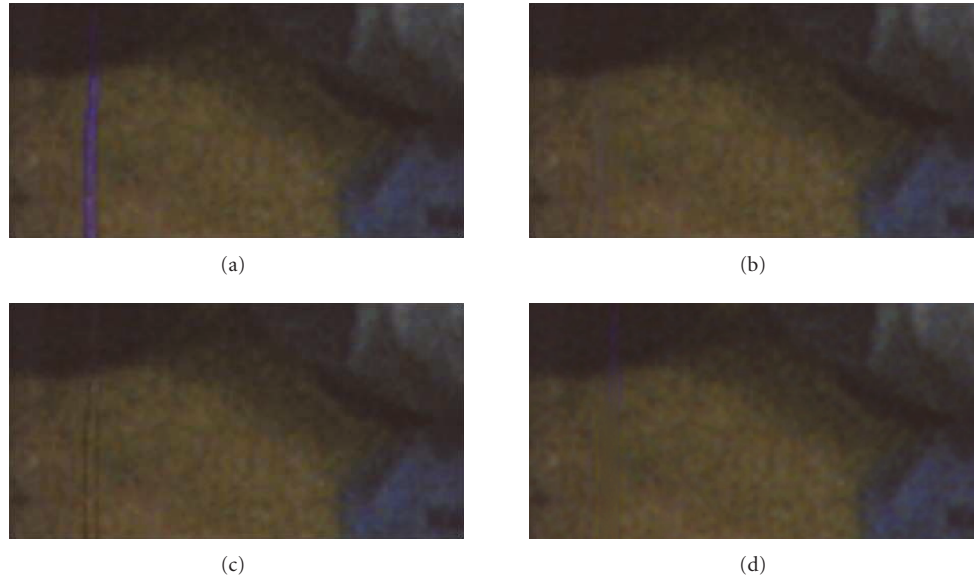


FIGURE 9: Zoom of the blue scratch in Figure 2(a) restored using the proposed algorithm (b), the method in [12] (c), and the method in [7] (d).

impulsive nature. For that reason, the approaches in [1, 7] create a blurred restored image.

The proposed approach does not introduce false colors, as it can be observed in the restoration of a blue scratch in Figure 9. The better performance of the proposed algorithm, in this case, is due to the fact that also the red component is restored. In fact, this scratch has a visible contribution on this component that is neglected by the approach in [12]. It is also worth noticing that the two thin dark lines near the scratch are not present in the image restored using the proposed model, thanks to a precise detection (three scratches are detected instead of a single one).

With regard to the computational effort, it is lower than most of the state-of-the-art techniques. In fact, as the approach in [12], the algorithm uses simple and fast computations, while it avoids expensive operations like the pixel-wise search of the best coherent block employed in [7], or correlation matrices, as in [1]. For a scratch occupying all the vertical extension of a 2 K frame (1828×1462 pixels), the restoration algorithm requires 2 seconds on a machine with a 2 GHz processor and a 1 G Ram, in a nonoptimized Matlab code.

Finally, the algorithm does not require any user's interaction since it is able to adapt both detection and restoration phases to the analyzed image.

6. CONCLUSIONS

In this paper a unified model for detection and restoration of line scratches on color movies has been presented. The model considers light diffraction and human perception to guide the reduction of the defect contribution in the image till it is masked by the local context. The resulting framework improves the performances of the available restoration approaches requiring a low computational effort.

Future research will be oriented to deal with more critical cases, such as scratches on highly textured areas or heavily degraded images. Moreover, efficient methods for false-alarms rejection will also be investigated.

ACKNOWLEDGMENTS

This paper has been partially supported by the FIRB project no. RBNE039LLC, "A knowledge-based model for digital restoration and enhancement of images concerning archaeological and monumental heritage of the Mediterranean coast." Authors would like to thank Sacher Film s.r.l. for providing the frames used in this paper, and Franco Strappini and Mario Musumeci of Centro Sperimentale di Cinematografia, Cineteca Nazionale (Rome) for their helpful suggestions and insightful comments.

REFERENCES

- [1] A. C. Kokaram, *Motion Picture Restoration: Digital Algorithms for Artefact Suppression in Degraded Motion Picture Film and Video*, Springer, Berlin, Germany, 1998.
- [2] L. Rosenthaler and R. Gschwind, "Restoration of movie films by digital image processing," in *Proceedings of IEE Seminar on Digital Restoration of Film and Video Archives*, pp. 6/1–6/5, London, UK, January 2001.
- [3] B. Besserer and C. Thiré, "Detection and tracking scheme for line scratch removal in an image sequence," in *Proceedings of the 8th European Conference on Computer Vision (ECCV '04)*, vol. 3023 of *Lecture Notes in Computer Science*, pp. 264–275, Prague, Czech Republic, May 2004.
- [4] T. Bretschneider, O. Kao, and P. J. Bones, "Removal of vertical scratches in digitised historical film sequences using wavelet decomposition," in *Proceedings of the Image and Vision Computing New Zealand (IVCNZ '00)*, pp. 38–43, Hamilton, New Zealand, November 2000.

- [5] V. Bruni, D. Vitulano, and A. Kokaram, "Fast removal of line scratches in old movies," in *Proceedings of the 17th International Conference on Pattern Recognition (ICPR '04)*, vol. 4, pp. 827–830, Cambridge, UK, August 2004.
- [6] V. Bruni and D. Vitulano, "A generalized model for scratch detection," *IEEE Transactions on Image Processing*, vol. 13, no. 1, pp. 44–50, 2004.
- [7] M. K. Gulu, O. Urhan, and S. Erturk, "Scratch detection via temporal coherency analysis and removal using edge priority based interpolation," in *Proceedings of IEEE International Symposium on Circuits and Systems (ISCAS '06)*, pp. 4591–4594, Kos Island, Greece, May 2006.
- [8] M. Haindl and J. Filip, "Fast restoration of colour movie scratches," in *Proceedings of the 16th International Conference on Pattern Recognition (ICPR '02)*, vol. 3, pp. 269–272, Quebec, Canada, August 2002.
- [9] L. Joyeux, S. Boukir, and B. Besserer, "Film line scratch removal using Kalman filtering and Bayesian restoration," in *Proceedings of the 5th IEEE Workshop on Applications of Computer Vision (WACV '00)*, pp. 8–13, Palm Springs, Calif, USA, December 2000.
- [10] L. Joyeux, O. Buisson, B. Besserer, and S. Boukir, "Detection and removal of line scratches in motion picture films," in *Proceedings of IEEE Computer Society Conference on Computer Vision and Pattern Recognition (CVPR '99)*, vol. 1, p. 553, Fort Collins, Colo, USA, June 1999.
- [11] G. Laccetti, L. Maddalena, and A. Petrosino, "Parallel/distributed film line scratch restoration by fusion techniques," in *Proceedings of the International Conference on Computational Science and Its Applications (ICCSA '04)*, vol. 3044 of *Lecture Notes in Computer Science*, pp. 525–535, Assisi, Italy, May 2004.
- [12] L. Maddalena and A. Petrosino, "Restoration of blue scratches in digital image sequences," Tech. Rep. 21, ICAR-NA, Napoli, Italy, December 2005.
- [13] L. Tenze and G. Ramponi, "Line scratch removal in vintage film based on an additive/multiplicative model," in *Proceedings of IEEE-EURASIP Workshop on Nonlinear Signal and Image Processing (NSIP '03)*, Grado, Italy, June 2003.
- [14] S. Winkler, *Digital Video Quality: Vision Models and Metrics*, John Wiley & Sons, New York, NY, USA, 2005.
- [15] M. Bertalmio, G. Sapiro, V. Caselles, and C. Ballester, "Image inpainting," in *Proceedings of the 27th International Conference on Computer Graphics and Interactive Techniques (SIGGRAPH '00)*, pp. 417–424, New Orleans, La, USA, July 2000.
- [16] S. Esedoglu and J. Shen, "Digital inpainting based on the Mumford-Shah-Euler image model," *European Journal of Applied Mathematics*, vol. 13, no. 4, pp. 353–370, 2002.
- [17] D. Kincaid and W. Cheney, *Numerical Analysis*, Brooks Cole, Florence, Ky, USA, 2002.